Int J Adv Manuf Technol (2010) 50:127–135
DOI 10.1007/s00170-009-2513-x

ORIGINAL ARTICLE

Evaluation of crack nucleation site and mechanical properties for friction stir welded butt joint in 2024-T3 aluminum alloy

Takao Okada · Masako Suzuki · Haruka Miyake · Toshiya Nakamura · Shigeru Machida · Motoo Asakawa

Received: 17 August 2009 / Accepted: 30 December 2009 / Published online: 2 February 2010

Abstract In this paper, metallographic observations, hardness measurement, and static and fatigue tests were conducted to investigate the discontinuity states which become crack nucleation sites in friction stir welded butt joints in 2-mm-thick 2024-T3 aluminum alloy and static and fatigue properties of the joint. Because different types of surface finish can be used depending on the application of the joint, several types of surface conditions were tested to evaluate their effect on crack nucleation sites and static and fatigue life. Indentation hardness tests revealed that typical hardness reduction is not necessarily observed on the section of the welding line. Based on fatigue test results, it was confirmed that there are several types of crack nucleation sites for friction stir welding (FSW) joints depending on the surface finish, and the features of the fracture surface also differ depending on the site. Furthermore, the type of discontinuity state affects the fatigue life of the FSW joint.

Keywords Friction stir welding · Fatigue strength · Aluminum alloy · Nucleation site

T. Okada (✉) · T. Nakamura · S. Machida
Aviation Program Group, Japan Aerospace Exploration Agency,
6-13-1 Osawa,
Mitaka, Tokyo 181-0015, Japan
e-mail: okada.takao@jaxa.jp

M. Suzuki · H. Miyake · M. Asakawa
Waseda University,
3-4-1 Okubo,
Shinjuku, Tokyo 169-8555, Japan

1 Introduction

Friction stir welding (FSW) is a relatively novel joining technique invented by TWI in 1991. Its application has spread to many structures such as for automobiles, trains, rockets, and ships. Although there have been many research activities to evaluate the properties of FSW to further expand its application, these have usually used a plate thickness of 6 mm or more [1–3]. However, this is thicker than the plate thickness for many aircraft structures.

For commercial aircraft, FSW was firstly applied to the nose barrier beam of the Boeing 747 freighter [4], but this component is not fatigue critical, and the use of FSW for fatigue critical components is indispensable to expand its application to aircraft. Eclipse Aviation Corporation first applied FSW to primary structures in the Eclipse 500 small business jet [5], where it was used for lap-type joints such as connections between the skin and stringers in the wing and fuselage. The mechanical properties of an FSW skin-stringer panel were also investigated by Sato et al. [6]. The FSW butt joint as an alternative to the conventional riveted lap joint has weight and cost-saving benefits, and other companies are also planning to apply FSW to transport category aircraft [7]. However, primary aircraft structure has to comply with damage tolerant requirements, particularly in transport category aircraft. Therefore, a way for thin FSW butt joints to comply with damage tolerance requirements is a topic of intensive research [8–10].

However, some researchers point out that damage tolerance alone is not sufficient to establish the structural integrity of aircraft structures. It has been found that the selection of initial discontinuity size has a large effect on the evaluation of fatigue life and hence on decisions relating to inspection intervals [11]. Therefore, holistic life prediction that includes the effects of the environment and

Table 1 Chemical composition of 2024-T3 aluminum alloy (mass %)

	Si	Fe	Cu	Mn	Mg	Cr	Zn	Ti
Composition	0.5 max	0.5 max	3.8 min 4.9 max	0.3 min 0.9 max	1.2 min 1.8 max	0.1 max	0.2 max	0.1 max

the heterogeneity of the material is imperative to provide the necessary structural integrity for aircraft structures [12]. In this method, a subset of the initial discontinuity state (IDS)/modified discontinuity state act as crack nucleation sites. Based on this circumstance and progress in engineering technology, research is being conducted into the IDS of materials used in aircraft structures [13].

In the case of FSW joints, the microstructure in the welding line is different from that in the base material. The treatment of tool marks and burrs during the FSW process varies depending on the applied location. Furthermore, the crack nucleation sites of the joint may vary with the joint type, such as butt, shear lap, or hard point. Therefore, the evaluation of discontinuity states in FSW joints is indispensable for their holistic life prediction.

In this research, measurements of micro- and macrostructure, micro-indentation hardness test, and static and fatigue tests were carried out on FSW butt joints in 2-mm-thick aluminum alloy to investigate the discontinuity states which become crack nucleation sites for the joint.

2 Experimental procedure

The 2024-T3 aluminum alloy specimens used in this evaluation had dimensions of 2 mm thickness, 150 mm width, and 500 mm length. The chemical composition is shown in Table 1. The FSW butt joints were fabricated by a Japanese manufacturer. The rolling direction of the plates is parallel to the direction of the friction stir weld.

2.1 Metallographic observation

Metallographic observations of the joints were conducted to investigate the microstructure in the welding area. The surface was first ground and then polished with deagglomerated alumina paste up to 0.05 μm. A commercial etching reagent and Keller solution (ASTM E-407) were used to observe the overall metallographic features and the detailed microstructure of the welding area, respectively. Sections parallel and perpendicular to the welding line were observed.

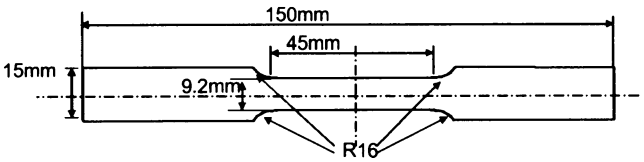

Fig. 1 Specimen geometry used for static tests

2.2 Hardness test

The hardness distribution in the welding area was measured to predict the probable crack nucleation sites of the joint. The surface treatment before the hardness test was same as that for the metallographic observation. The micro-indentation hardness test procedure (ASTM E-384) was employed. Because the width of each zone (weld nugget, thermo-mechanically affected zone (TMAZ), heat affected zone (HAZ) and base material) will differ depending on the thickness direction of the plate, the hardness profile was measured at 0.5, 1.0, and 1.5 mm in the thickness direction from the bottom of the plate. The indentation force was set to 9.8 N.

2.3 Static and fatigue tests

Static load tests were conducted to evaluate the yield and ultimate strength of the FSW joints. The specimen geometry is shown in Fig. 1. Specimens were cut out from an FSW panel such that the welding direction was perpendicular to the loading direction, and the welding line was located at the center of the specimen. The specimen was loaded in the T-direction. Specimens with tangentially blended fillets were used for the fatigue test. The specimen dimensions are shown in Fig. 2. The fatigue specimens were cut out from the FSW panel in the same way as for the static specimens.

Two types of surface finish were used to evaluate the effect of surface finish on joint static strength. And four

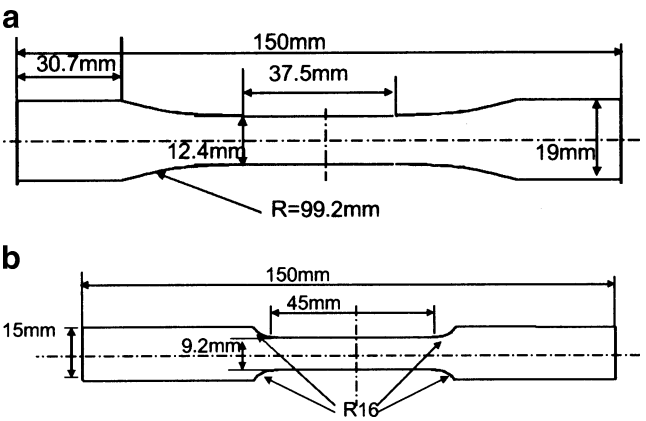

Fig. 2 Specimen geometry used for fatigue tests. **a** As weld and both surface grinding. **b** Top surface polished and both surface polished

types of surface finish were used to evaluate the effect of surface finish on crack nucleation site and joint fatigue life. The first condition is no surface additional treatment and is named “as weld” in this paper. The test results for this condition will show the effects of tool marks, burrs, and lack of penetration (LOP) [14], which is referred to as kissing bond or root flaw [15] by some researchers, on fatigue properties. The second condition is 0.2 mm grinding of both the top and bottom surfaces and is named “both surface grinding”. Surface grinding may be applied to welded surfaces because it is difficult to apply paint to areas with tool marks and burrs, so the effect of surface finish by a machining process is evaluated. For the third condition, named “top surface polished”, only the top surface was polished to clarify the effect of the LOP of the specimen. For the last condition, named “both surfaces polished”, both surfaces of the specimen were first ground and then polished with alumina paste up to 0.05 μm to exclude the effects of tool marks, burrs, and LOP on crack nucleation. For all specimens, the treatment of the specimen side was same as that of the polished surface to prevent fracture due to surface roughness during specimen preparation.

The specimens were subjected to cyclic loading with R=0.1 and f=10 Hz. Three values of maximum stress, 200, 250, or 300 MPa, were used in this research. Tests were conducted at room temperature.

3 Test results

3.1 Metallographic observation

Figure 3 shows an optical micrograph and EBSD image of a section. In the base material, smaller microstructure is observed near the surface because of its manufacturing process. In the weld nugget, the average size of the equiaxed grain structure is approximately 0.8 μm. It is confirmed that the weld nugget does not reach to the bottom of the joint. Measurement of the joint microstructure reveals a periodic feature in the metallic structure in the section parallel to the welding line, and its pitch is close to the ratio of the tool traveling speed to the tool rotation speed. The ratio is 0.51 mm/rpm for this welding condition. The measured pitch of the tool marks is also same as this ratio.

3.2 Hardness test

Figure 4 shows the hardness distribution in a section perpendicular to the welding line and an optical micrograph of the section together with the tool dimension. The average hardness values of the base material in the middle and near the surface are 127 and 137 HV, respectively. From this figure, it is considered that there is no typical hardness drop

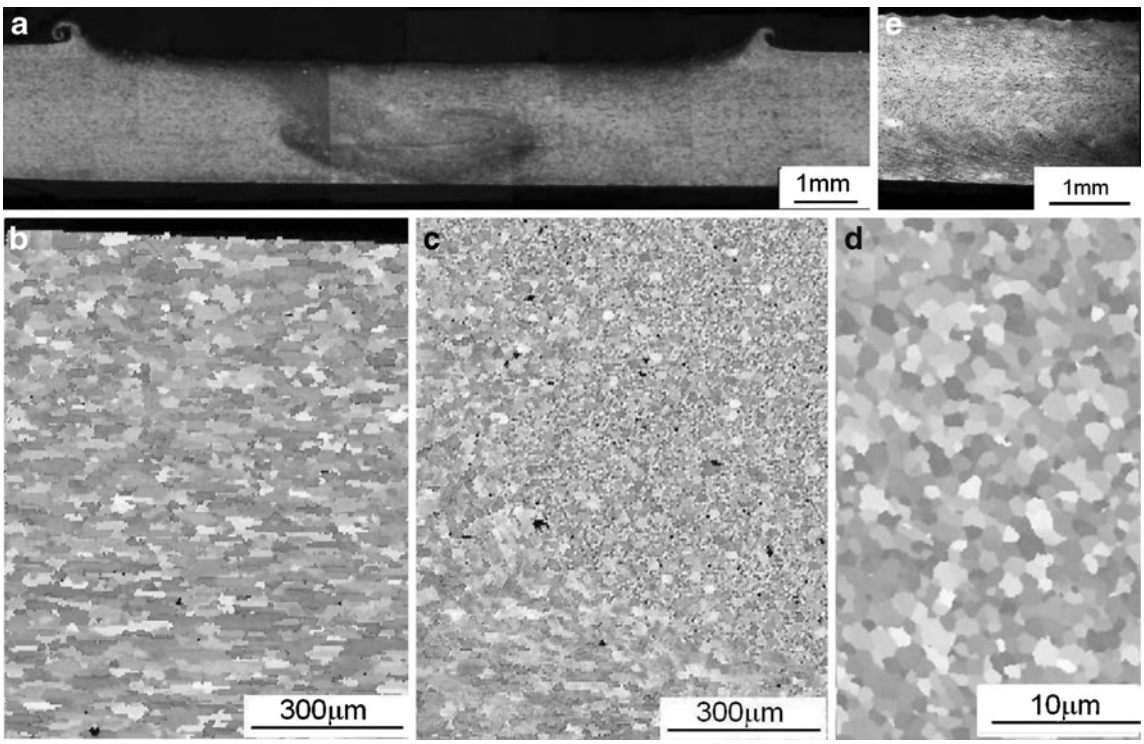

Fig. 3 Metallographic observations of sections. **a** Section perpendicular to the welding line. **b** Base material, **c** TMAZ/SZ boundary. **d** SZ. **e** Section parallel to the welding line

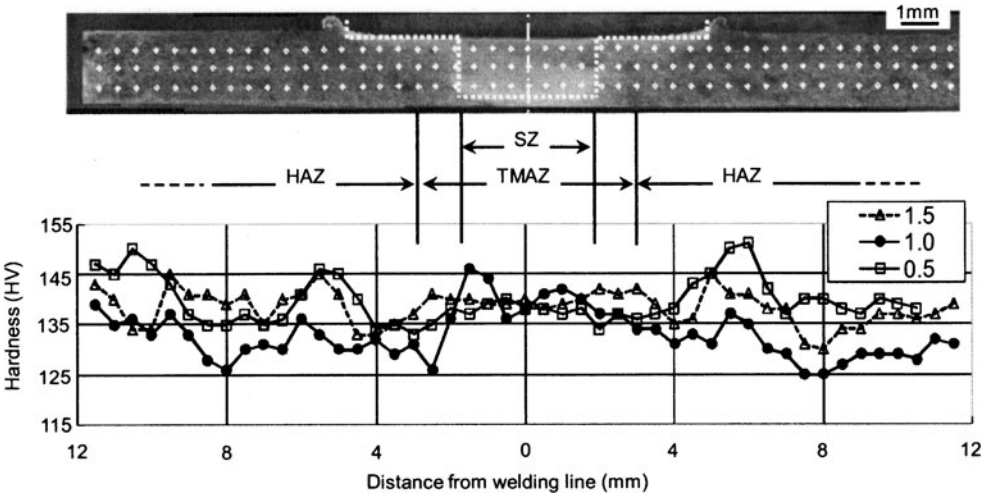

Fig. 4 Hardness profile on welding line

region in this welding condition. Also, it appears that the hardness distribution through the thickness direction does not significantly change in the base material and HAZ. However, in the TMAZ and the weld nugget, plastic flow and heat input change the thickness hardness distribution.

3.3 Static and fatigue tests

Table 2 shows the static test results for the base material and the as weld specimen. Five specimens are tested for each condition. As shown in the table, the average yield strength of the as weld specimen is 319.6 MPa, 6% higher than that of the base material, while its ultimate strength is 435.2 MPa, 10% lower than that of the base material. As described later, FSW joint for this welding condition has the LOP. It becomes the origin of the static failure of as weld specimen and decreases the ultimate strength. By removing the LOP, the ultimate strength of the FSW joint improves to that of the base material.

Figure 5 shows the S–N data for the FSW specimens. The test results for the base material with the as-received surface condition are also shown in the figure. The average fatigue life and variation coefficient for each condition are summarized in Table 3. This figure shows that the fatigue properties of the "as weld" specimens are apparently lower than those of the base material. The specimens fractured at about 170,000 cycles at the maximum stress of 200 MPa, while the base material indicates run-out (2,000,000 cycles) at 250 MPa. Most of the specimens fractured in a vicinity of a burr as shown in Fig. 6. In other cases, an LOP becomes the crack nucleation site (Fig. 7). The average fatigue cycles for "both surface grinding" specimens are about an order of magnitude greater than for the "as weld" specimens. However, only one specimen reaches run-out in this test, and then, the fatigue property of the FSW joint for the condition is not the same as that of the base material.

Figure 8 shows the fracture surface of a specimen which fractured at the lowest fatigue cycles. The crack origin appears to be a crevice located inside the specimen. Other specimens fractured at the end point of the gauge length or at a grinding mark caused by the mechanical grinding process (Fig. 9). The fatigue performance of "top surface polished" specimens is even lower than of "as weld" specimens at the maximum stress of 250 MPa. Similarly to one of the "as weld" specimens, the LOP is the crack origin in this case. The fatigue cycles of "both surfaces polished" specimens show wide variation. The shortest fatigue life is the same order of magnitude as the fatigue life of "as weld" specimens, while the longest are more than the 2,000,000 cycles which is the value set as the run-out cycles for the base material. In cases where the fatigue cycle is longer than the run-out, the fatigue crack originated from inside the specimen. In other cases, a particle was the crack origin.

4 Discussion

Several types of fracture surface were observed, and some types of discontinuity states were identified depending on the surface finish.

Table 2 Static test results

	Yield strength		Tensile strength	
	Average	Variation coefficient	Average	Variation coefficient
Base material	319.6	0.0134	482.0	0.0025
FSW (as weld)	339.4	0.0085	435.2	0.0518
FSW (both surface grinding)	355.4	0.0160	483.0	0.0207

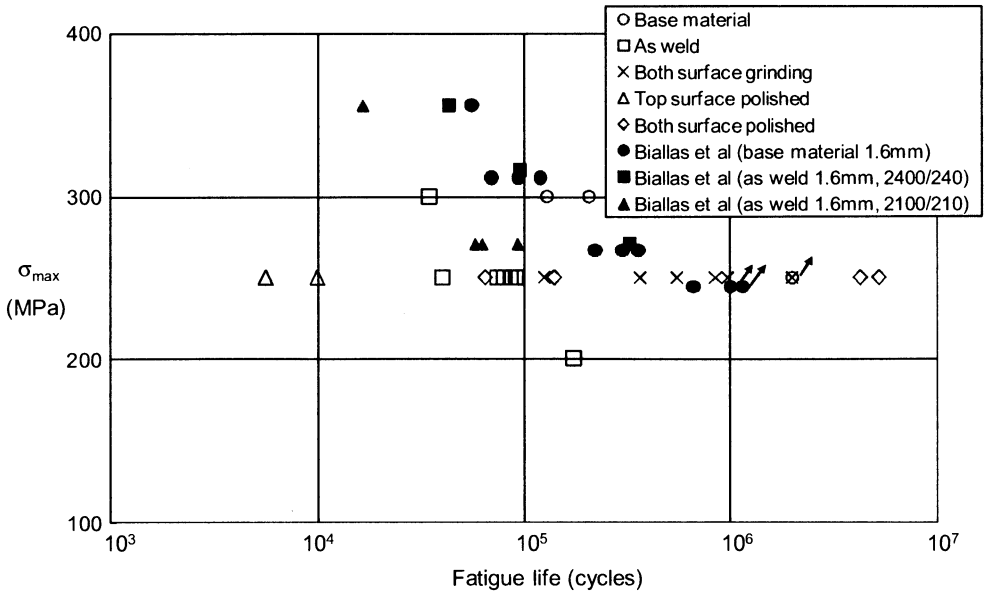

Fig. 5 Fatigue test result

4.1 "As weld" condition

Tool marks near the burrs and the LOP are considered as origins for "as weld" specimens. As observed on some fracture surfaces, multiple cracks start at multiple locations at the tool marks and link up to form a large crack. This indicates that multiple crack starters are distributed along the welding line. Therefore, tool marks near the burr are detrimental to the fatigue properties of FSW joints in this welding condition. The heights of the burr and the tool marks for the specimens used in this paper were about 0.45 and 0.05 mm, respectively, and the thickness reduction at the welding line was about 0.15 mm. In addition, the fracture location was in the vicinity of a burr for all specimens (Fig. 6a), in cases where tool marks were the crack origins. It is thus considered that stress concentration by the burrs and tool marks causes the formation of cracks.

In [9], concentric ripples above the SZ or roll scratches below it became crack nucleation sites for an FSW butt joint with 1.6 mm thickness, rather than tool marks near the burr, because of thickness reduction during the welding process. The height of the burr was 0.07 mm at most in that case. Several data from this reference are also indicated in Fig. 5. When thickness reduction is a key factor in the failure [tool rotation speed/tool travel speed=2,400 rpm/(240 mm/min)], the fatigue life is within the scatter band of the base material. Therefore, it is supposed that the crack nucleation sites and fatigue life could change significantly if the height of the burrs and the thickness reduction along the welding line increase.

The LOP also shows a detrimental effect on fatigue properties. It is located at the bottom side of the specimen along the center of the welding line. As shown in Fig. 7, the appearance of the fracture surface up to approximately 0.15 mm from the bottom side is quite different from that far from the bottom surface, and its features differ from those of fatigue failure of the base material. Because an LOP which has insufficient bonding has discontinuities, it will separate in the early stage of the fatigue life and acts as multiple crack nucleation sites.

The crevice shown in Fig. 8 acts as a fatigue crack origin for "both surface grinding" specimens. It locates about 2 mm away from the center of the welding line and within the track of the tool pin and is 1.45 mm wide, 0.4 mm high, and 0.1 mm deep. Its surface features appear to be in the form of laminae and differ from the appearance of fatigue failure. Therefore, this crevice seems to be a discontinuity state which was induced during the welding process. From the point of fatigue life, this type of crevice can also be a crack origin for "as weld" specimens. Other types of discontinuity state formed during the welding process were also observed by Biallas et al. [9]. They confirmed that pores located in the lower part of the SZ were a crack origin in the case that the tool rotation speed, and the tool traveling speed were 2,100 rpm and 210 mm/min, respectively. The size of a typical pore was 0.3 mm wide and 0.085 mm high. The fatigue life for this welding condition

Table 3 Average fatigue life and variation coefficient for each surface condition (σ_{max}=250 MPa)

	Average fatigue life	Variation coefficient
As weld	77,220	0.253
Both surface grinding	810,478	0.815
Top surface polished	7,831	2.552
Both surfaces polished	2,742,961	0.894

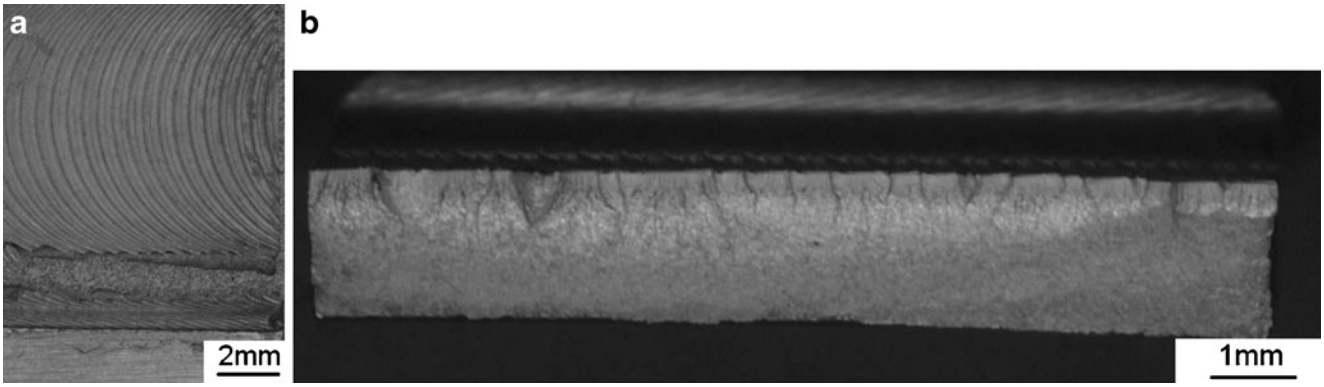

Fig. 6 Typical fracture surface in case multiple cracks form at tool mark. **a** Fracture location. **b** Fracture surface

is also shown in Fig. 5. It is shorter than that of the base material and 2400/240 joints, and the observed pores are considered to be detrimental to fatigue strength in that welding condition.

Based on these results, burrs, tool marks, and the LOP are the primary discontinuity states affecting the fatigue life for "as weld" specimens in this welding condition. The size in the thickness direction of the burrs, tool marks, and LOP were about 0.45 mm, 0.05 mm, and 0.15 mm, respectively. This seems small compared with the initial flaw size usually used for damage tolerant design (e.g., 1.27 mm). Their distribution along the welding line makes them critical to fatigue properties. In addition, crevices induced by the welding process need to be considered if any exist. The crevice size is 1.45 mm and is comparable to the initial flaw size.

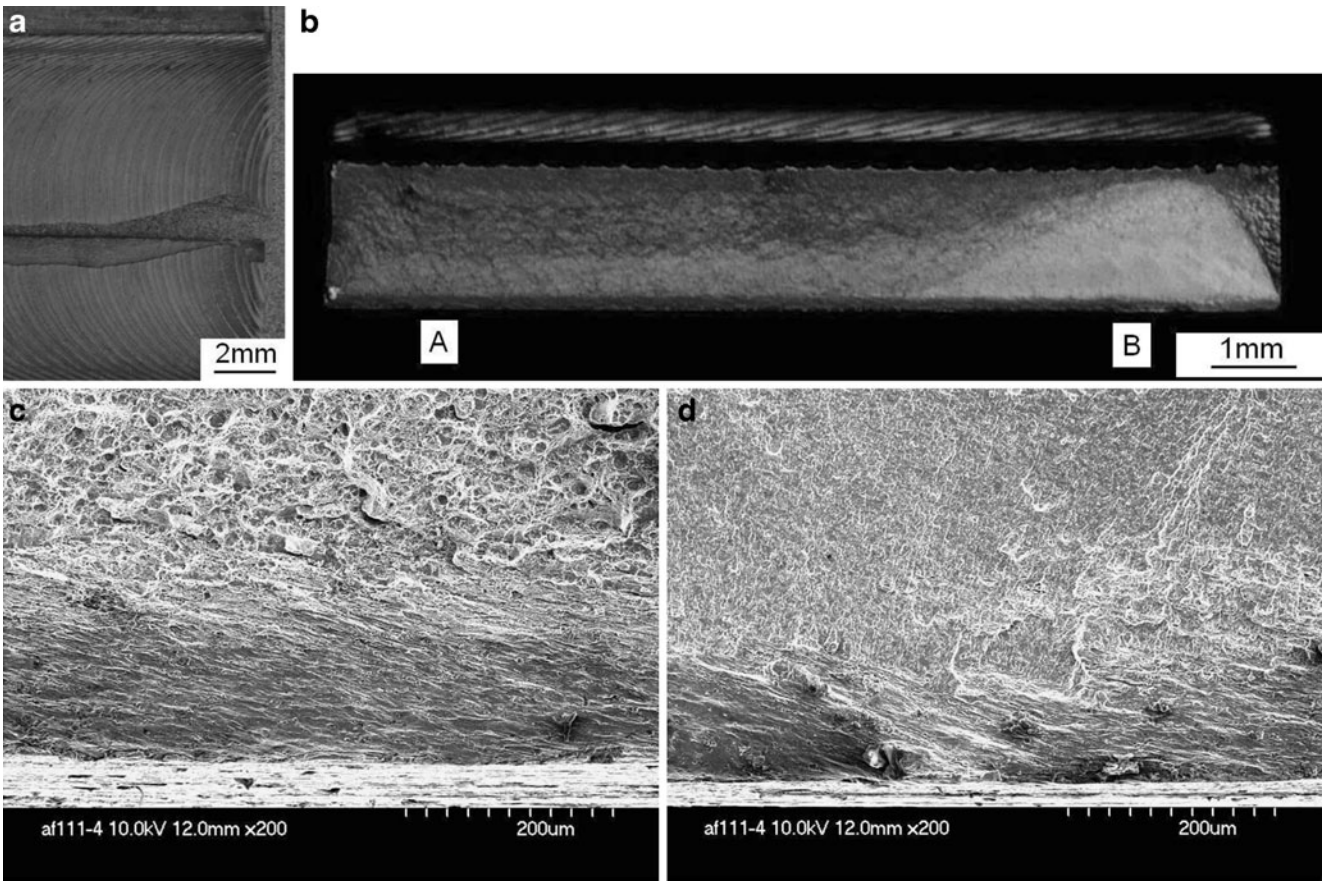

Fig. 7 Typical fracture surface when LOP is the crack origin. **a** Fracture location. **b** Fracture surface. **c** Fracture surface at point A. **d** Fracture surface at point B

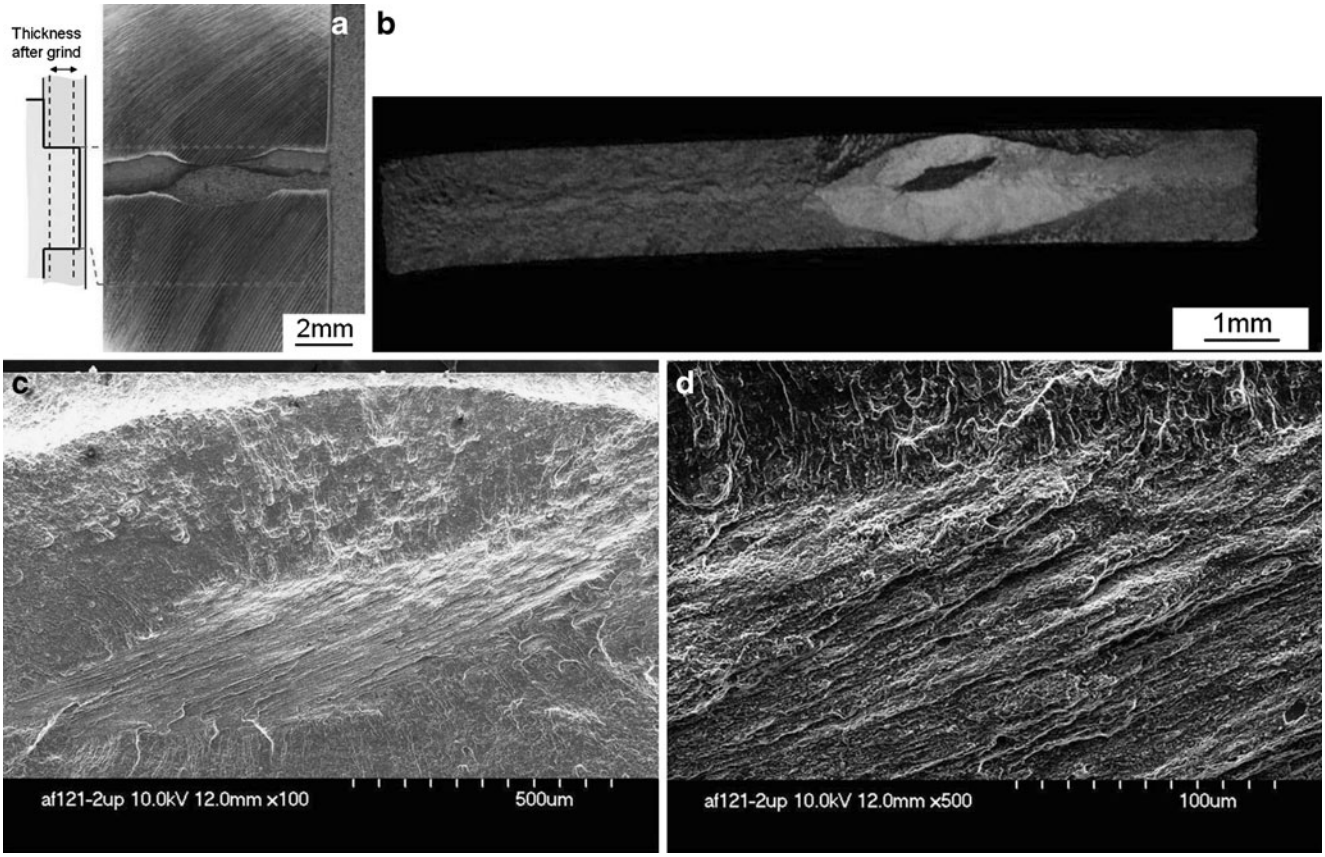

Fig. 8 Typical fracture surface when an internal crevice is the crack origin. **a** Fracture location. **b** Fracture surface. **c** Fracture surface around crevice. **d** Fracture surface around crevice

4.2 Both surface grinding condition

For the "both surface grinding" specimens, tool marks and the LOP are removed, and the mechanical grinding marks become a discontinuity state affecting fatigue life. If a crevice due to an inadequate welding process exists in the joint, it can be a more detrimental discontinuity state as identified in this test result. The surface roughness of the grinding marks, Ra, was 25 μm in this case and is smaller than discontinuity states identified for the "as weld" specimens. Therefore, a greater fatigue life is obtained.

4.3 Both surfaces polished condition

Two types of discontinuity states are observed for "both surfaces polished" specimens, where the LOP is removed. For the first type of fracture surface, the crack origin is on the surface. SEM observation identifies that a particle acts

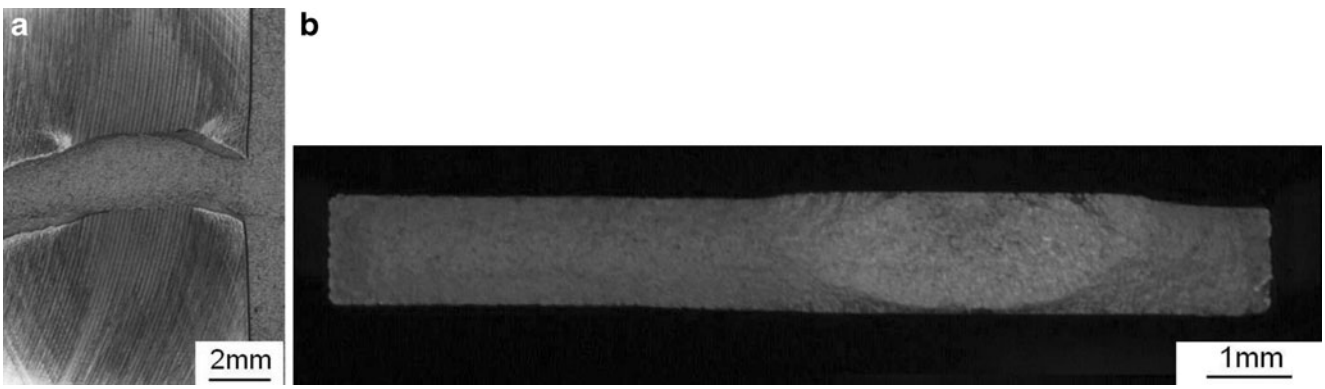

Fig. 9 Typical fracture surface when a grinding mark is the crack origin. **a** Fracture location. **b** Fracture surface

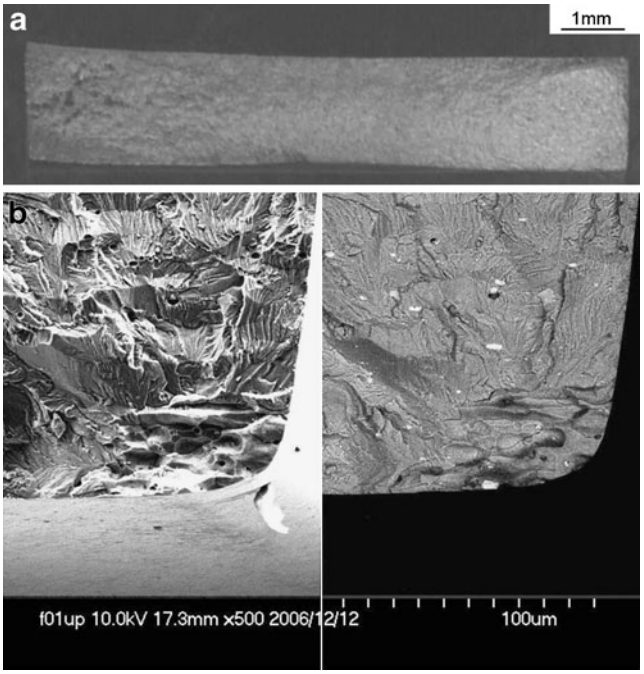

Fig. 10 Typical fracture surface in case particle is crack origin. **a** Fracture surface. **b** Fracture surface near origin

as a crack origin in this case (Fig. 10). These were located 5 and 15 mm away from the center of the welding line, not only in the base material but also in the HAZ. (Their sizes were 22 and 44 μm^2, respectively). In [13], the discontinuity state for 2024-T3 aluminum alloy was evaluated using a polished specimen, and particles on the surface were identified as crack origins. Therefore, similarly to the base material, particles in an FSW butt joint can become discontinuity states that affect fatigue life when other discontinuity states such as burrs and the LOP are removed.

The other type of crack origin was a crevice parallel to the loading direction located inside the specimen as shown in Fig. 11. It was located 5 mm away from the center of the welding line and outside of the track of the tool pin. Its size in the loading direction was about 1 mm, about an order of magnitude larger than the crevice observed in Fig. 8. The features of the fracture surface differ from fractures caused by an inadequate welding process, so the origin is not a flaw induced by an inadequate welding process. It is well known that an inclusion inside of specimen can become a crack origin for high cycle fatigue such as 10^7 cycles and higher. However, the inclusions which act as an origin are generally small and the fracture surfaces around them do not have a step as observed in Fig. 11. Therefore, this is different from high cycle fatigue fracture of the base

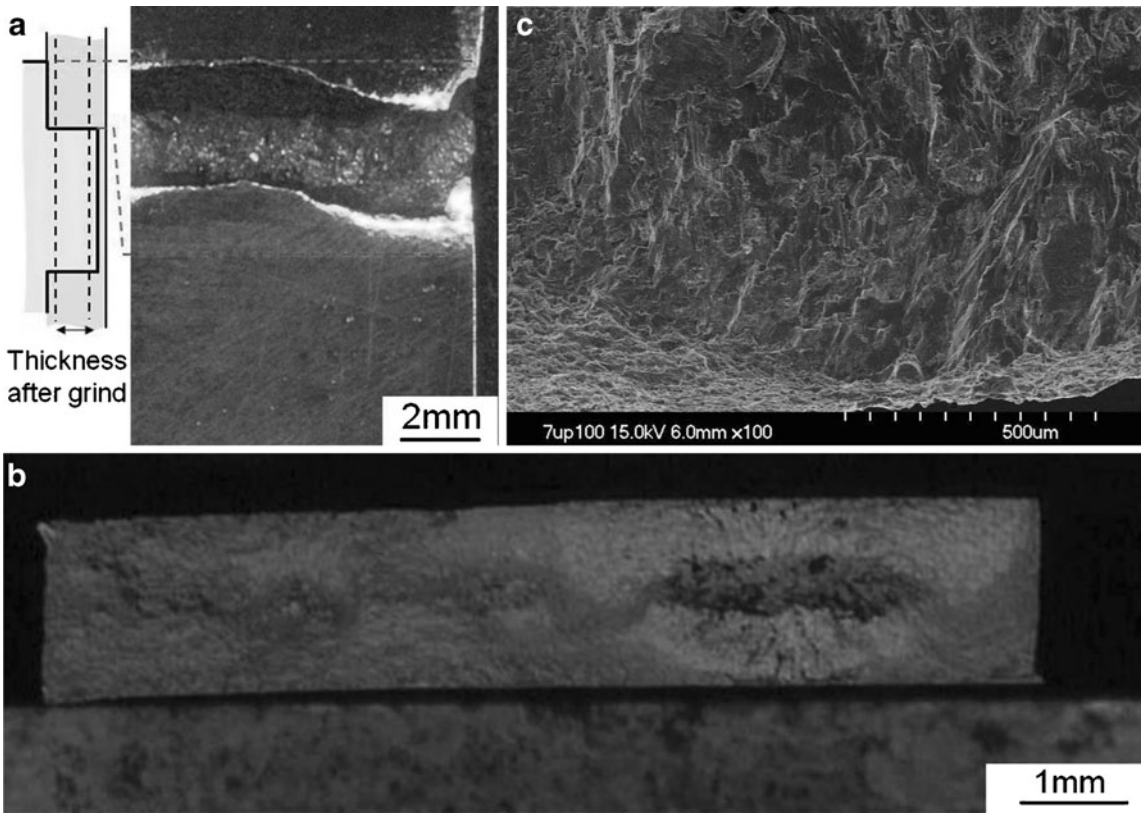

Fig. 11 Typical fracture surface in case crack forms at inside of specimen. **a** Fracture location. **b** Fracture surface. **c** Crevice surface

material. The reason for the formation of this type of origin is under investigation.

5 Conclusion

Metallographic observation, hardness distribution measurement, and static tests were conducted to evaluate the properties of an FSW butt joint in 2024-T3 aluminum alloy for this welding condition. Periodic features in the metallic structure were observed on the section parallel to the welding line with a pitch almost the same as the ratio of tool traveling speed to tool rotation speed and the same as the pitch of the tool mark. There was no typical hardness drop in the section perpendicular to the welding line in this welding condition.

Fatigue tests on the FSW joint were conducted to investigate the discontinuity states which become crack nucleation sites for several surface conditions. Several types of discontinuity states such as tool mark near the burrs, LOP, particles, etc., were observed depending on the surface finish. As has been shown in other papers, the critical discontinuity state was also affected by the welding condition. Based on the results, it was revealed that the type of these discontinuity states strongly affected the fatigue life of the FSW joint.

References

1. Bussu G, Irving PE (2003) The role of residual stress and heat affected zone properties on fatigue crack propagation in friction stir welded 2024-T351 aluminum alloy. Int J Fatigue 25:77–88. doi:10.1016/S0142-1123(02)00038-5
2. Dickerson TL, Przydatek J (2003) Fatigue of friction stir welds in aluminum alloys that contain root flaws. Int J Fatigue 25:1399–1409. doi:10.1016/S0142-1123(03)00060-4
3. Pao PS, Gill SJ, Feng CR, Sankaran KK (2001) Corrosion-fatigue crack growth in friction stir welded Al 7050. Scr Mater 45:605–612. doi:10.1016/S1359-6462(01)01070-3
4. Burford DA (2003) Friction stir welding of airframe structure: from one delivery system to another: SAE technical paper 2003-01-2897. SAE International, Warrendale
5. Dawes CJ (2003) Developing a metal joining process for fabricating airframes: AIAA-2003-2769. American Institute of Aeronautics and Astronautics, Reston
6. Sato H, Yamada Y, Tanoue Y (2007) Improvement of crack propagation properties of friction stir welded panels. In: Lazzeri L, Salvetti A (eds) ICAF 2007, durability and damage tolerance of aircraft structures: metals and composites, proceedings of the 24th symposium of the ICAF, Naples. Pacini, Pisa, pp 163–171
7. Schmidt HJ, Voto C, Hansson J (2001) TANGO metallic fuselage barrel validation of advanced technologies. In: Rouchon J (ed) ICAF 2001, design for durability in the digital age, proceedings of the 21st symposium of the ICAF, Toulouse. Cepadues-Editions, Toulouse, pp 273–288
8. Lemmen HJK, Alderliesten RC, Homan JJ, Benedictus R (2007) Design principles for damage tolerant butt welded joints for application in the pressurized fuselage. In: Lazzeri L, Salvetti A (eds) ICAF 2007, durability and damage tolerance of aircraft structures: metals and composites, proceedings of the 24th symposium of the ICAF, Naples. Pacini, Pisa, pp 147–162
9. Biallas G, Donne CD, Juricic C (2000) Monotonic and cyclic strength of friction stir welded aluminum joints. In: Miannay D et al (eds) Advances in mechanical behaviour. Plasticity and damage. Elsevier science, Kidlington, pp 115–120
10. Irving PE, Ma YE, Zhang X, Servetti G, Williams S, Moore G, dos Santos J, Pacchione M (2009) Control of crack growth rates and crack trajectories for enhanced fail safety and damage tolerance in welded aircraft structures. In: Bos MJ (ed) ICAF 2009, bridging the gap between theory and operational practice, proceedings of the 25th symposium of the ICAF, Rotterdam. Springer, Dordrecht, pp 387–405. doi:10.1007/978-90-481-2746-7_23
11. Liao M, Bellinger NC, Forsyth DS, Komorwski JP (2005) A new probabilistic damage tolerance analysis tool and its application for corrosion risk analysis. In: Dalle Donne C (ed) Structural integrity of advance aircraft and life extension for current fleets—lessons learned in 50 years after the comet accidents, proceedings of the 24th symposium of the ICAF, Hamburg. DGLR, Bonn, pp 241–252
12. Hoeppner DW (1985) Parameters that input to application of damage tolerance concepts to critical engine components. In: Asquith et al (eds) AGARD-CP-393: damage tolerance concepts for critical engine components. Advisory Group for Aerospace Research and Development, Neuilly-sur-Seine, pp 4/1–4/16
13. Merati A (2005) A study of nucleation and fatigue behavior of an aerospace aluminum alloy 2024-T3. Int J Fatigue 27:33–44. doi:10.1016/j.ijfatigue.2004.06.010
14. Pacchione M, Werner S, Ohrloff N (2007) Design principles for damage tolerant butt welded joints for application in the pressurized fuselage. In: Lazzeri L, Salvetti A (eds) ICAF 2007, durability and damage tolerance of aircraft structures: metals and composites, proceedings of the 24th symposium of the ICAF, Naples. Pacini, Pisa, pp 224–240
15. Threadgill PL, Leonard AJ, Shercliff HR, Withers PJ (2009) Friction stir welding of aluminum alloys. Int Mater Rev 54:49–93. doi:10.1179/174328009X411136